

Characteristics of a Miniature Compartment-less Glucose–O₂ Biofuel Cell and Its Operation in a Living Plant

Nicolas Mano, Fei Mao, and Adam Heller

J. Am. Chem. Soc., **2003**, 125 (21), 6588-6594 • DOI: 10.1021/ja0346328 • Publication Date (Web): 30 April 2003

Downloaded from <http://pubs.acs.org> on March 28, 2009



More About This Article

Additional resources and features associated with this article are available within the HTML version:

- Supporting Information
- Links to the 24 articles that cite this article, as of the time of this article download
- Access to high resolution figures
- Links to articles and content related to this article
- Copyright permission to reproduce figures and/or text from this article



[View the Full Text HTML](#)



Characteristics of a Miniature Compartment-less Glucose–O₂ Biofuel Cell and Its Operation in a Living Plant

Nicolas Mano,^{*,†} Fei Mao,[‡] and Adam Heller^{*,†}

Contribution from the Department of Chemical Engineering and Texas Materials Institute, The University of Texas at Austin, Austin, Texas 78712, and TheraSense Inc., 1360 South Loop Road, Alameda, California 94502

Received February 12, 2003; E-mail: heller@che.utexas.edu; mano@mail.utexas.edu

Abstract: We report the temperature, pH, glucose concentration, NaCl concentration, and operating atmosphere dependence of the power output of a compartment-less miniature glucose–O₂ biofuel cell, comprised only of two bioelectrocatalyst-coated carbon fibers, each of 7 μm diameter and 2 cm length (Mano, N.; Mao, F.; Heller, A. *J. Am. Chem. Soc.* **2002**, *124*, 12962). The bioelectrocatalyst of the anode consists of glucose oxidase from *Aspergillus niger* electrically “wired” by polymer I, having a redox potential of –0.19 V vs Ag/AgCl. That of the cathode consists of bilirubin oxidase from *Trachyderma tsunodae* “wired” by polymer II having a redox potential of +0.36 V vs Ag/AgCl (Mano, N.; Kim, H.-H.; Zhang, Y.; Heller, A. *J. Am. Chem. Soc.* **2002**, *124*, 6480. Mano, N.; Kim, H.-H.; Heller, A. *J. Phys. Chem. B* **2002**, *106*, 8842). Implantation of the fibers in the grape leads to an operating biofuel cell producing 2.4 μW at 0.52 V.

Introduction

The anode and cathode compartments of most fuel cells are separated by an ion-conducting membrane. In the most widely used H₂–O₂ cell, hydrogen is oxidized to water at the anode at a reducing potential and oxygen is reduced to water at the cathode at an oxidizing potential. In the phosphoric acid electrolyte H₂–O₂ cell, a Nafion membrane excludes oxygen from the anode compartment and hydrogen from the cathode compartment.^{1–3} Because the anode is poised at a reducing potential with respect to the cathode and because both the anode and the cathode comprise platinum group metal catalysts, without a membrane hydrogen would be more readily oxidized at the cathode, and oxygen would be more readily reduced at the anode. As a result, the power output would be nil or negligibly small. In all but a few of the earlier reported biofuel cells, the anode and cathode compartments were also separated by an ion-exchange membrane.^{4–11} In cells having platinum group metal-

based O₂ cathodes, separation was necessary because the anodic reactant's electrooxidation products poisoned the metallic platinum group electrocatalyst of the cathode.^{4–7} In cells containing a dissolved redox mediator in the anode compartment, to transport electrons from its substrate-reduced oxidase or dehydrogenase to the anode, the membrane was essential to prevent electrooxidation of the mediator at the cathode. In cells containing a dissolved redox mediator in the cathode compartment, to transport electrons from the cathode to its O₂-oxidized laccase or other enzyme, the membrane was essential to prevent reduction of the mediator at the anode.^{8–13}

The electrocatalysts of this study are “wired” enzymes.^{14,15} They are electrostatic adducts of redox enzymes, which are polyanions at neutral pH, and electron-conducting redox polymers, which are polycations. The adduct prevents phase separation of the redox polymer and the enzyme. The redox potential of polymer I “wiring” the anodic enzyme (Figure 1, top), glucose oxidase (GOx), is tailored to be just slightly oxidizing with respect to the redox potential of GOx, and polymer II (Figure 1, bottom) “wiring” the cathodic enzyme, bilirubin oxidase (BOD), is just slightly reducing with respect to the potential of BOD. This provides for an electron cascade in the direction glucose → glucose oxidase → polymer I → anode → external resistance → cathode → polymer II → BOD → O₂. The external resistance, rather than the kinetic resistance of any of the six electron-transfer steps, dominates the potential difference between glucose and O₂ (Scheme 1). By basing the

[†] The University of Texas at Austin.

[‡] TheraSense Inc.

- (1) Hillman, A. R. In *Electrochemical science and technology of polymers*; Linford, R. G., Ed.; Elsevier: London, 1987; p 103.
- (2) *Fuel Cells and Their Applications*; Kordesch, K., Simader, G., Eds.; VCH Publisher: New York, 1996; p 384.
- (3) Ormerod, R. M. *Chem. Soc. Rev.* **2003**, *32*, 17–28.
- (4) Appleby, A. J.; Ng, D. Y. C.; Weinstein, H. *J. Appl. Electrochem.* **1971**, *1*, 79–90.
- (5) Rao, J. R.; Richter, G.; Von Sturm, F.; Weidlich, E. *Ber. Bunsen-Ges. Phys. Chem.* **1973**, *77*, 787–790.
- (6) Wan, B. Y. C.; Tseung, A. C. C. *Med. Biol. Eng.* **1974**, *12*, 14–28.
- (7) Affrossman, S.; Courtney, J. M.; Gilchrist, T.; Martin, I. *Med. Biol. Eng.* **1975**, *13*, 539–543.
- (8) Turner, A. P. F.; Ramsay, G.; Higgins, I. J. *Biochem. Soc. Trans.* **1983**, *11*, 445–448.
- (9) Palmore, G. T.; Kim, H.-H. *J. Electroanal. Chem.* **1999**, *464*, 110–117.
- (10) Palmore, G. T.; Bertschy, H.; Bergens, S. H.; Whitesides, G. M. *J. Electroanal. Chem.* **1998**, *443*, 155–161.
- (11) Sasaki, S.; Karube, I. *Trends Biotechnol.* **1999**, *17*, 50–52.

- (12) Kang, C.; Xie, Y.; Anson, F. C. *J. Electroanal. Chem.* **1996**, *413*, 165–174.
- (13) Pizzariello, A.; Stred'ansky, M.; Miertus, S. *Bioelectrochemistry* **2002**, *56*, 99–105.
- (14) Heller, A. *Acc. Chem. Res.* **1990**, *23*, 128–134.
- (15) Heller, A. *J. Phys. Chem. B* **1992**, *96*, 3579–3587.

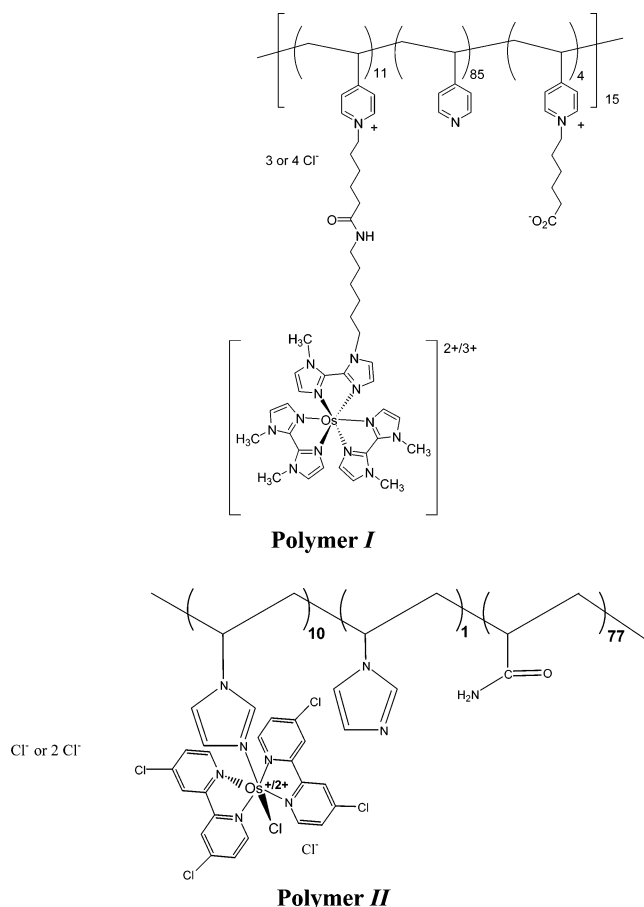
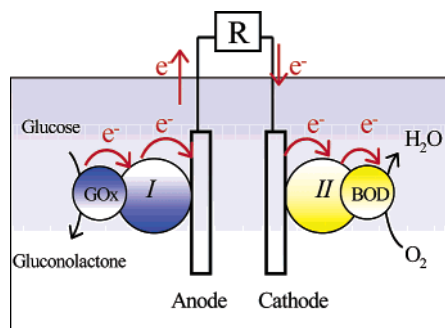


Figure 1. Structures of the anodic wire, polymer I, and of the cathodic wire, polymer II.

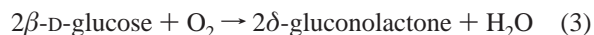
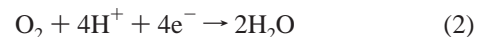
Scheme 1. Schematic Diagram of the Compartment-less Biofuel Cell^a



^a The two electrodes, coated with different cross-linked electrostatic adducts of enzymes and redox polymers, reside in the same solution. At the anode, electrons are transferred from glucose to glucose oxidase (GOx), from GOx to Os(III), and from Os(II) to the electrode. At the cathode, electrons are transferred from the cathode to Os(III), from Os(II) to BOD, and from BOD to O₂.

anode and cathode electrocatalysts on “wired” enzymes, it is possible to make both electrodes so selective for their respective reactants that the current-depleting oxidation of glucose at the cathode, and reduction of O₂ at the anode, are slower than the desired electrooxidation and electroreduction of reactants at their intended electrode. Beyond the key condition of selectivity, two additional conditions must be met in order to allow the elimination of the compartment-separating membrane: the readily poisoned platinum group metal catalysts must be avoided, and neither compartment may contain a dissolved redox mediator.

In the compartment-less biofuel cell (Scheme 1), the electrons of glucose reduce GOx, glucose being electrooxidized to δ -gluconolactone (eq 1). The electrons are collected and transported to the anode by redox polymer I. Electrons are transported from the cathode through redox polymer II to O₂-oxidized bilirubin oxidase, catalyzing its electroreduction of O₂ to water (eq 2). The overall cell reaction is represented by eq 3.



The current densities of the anode and the cathode of a biofuel cell based on the “wiring” of enzymes are limited by the amount and the turnaround rate of the enzyme that is “wired”. While in the H₂–O₂ and in the methanol–air fuel cells, which can be miniaturized and chip-mounted,¹⁶ the current densities are of hundreds of milliamperes per square centimeter, the current densities of smooth “wired” enzyme electrodes are only ~ 1 mA cm⁻² and reach only 2–10 mA cm⁻² when the electrodes are porous. Furthermore, the operational lives of the H₂–O₂ and methanol–air fuel cells are of years, while the operational lives of biofuel cells based on “wiring” of enzymes are ~ 1 week. Nevertheless, because the enzyme “wiring”-based cells are structurally simpler, are uniquely easy to miniaturize, and their electrodes are potentially mass-manufacturable at the same cost as glucose anodes used in glucose monitors for diabetes management ($< 10\text{¢}$), the cells are likely to be disposable and find applications. As the size of microelectronic circuits and sensors shrinks, the size of the low-power sensor–transmitter package (of potential value in physiological research and in medicine) becomes increasingly dependent on the size of its power source. The miniature biofuel cells are likely to meet the need for a small power source in low-power sensor–transmitter systems.

Earlier, progress toward a compartment-less biofuel cell anode was made by Persson and Gorton, who electrooxidized glucose on a carbon anode on which a redox mediator was chemisorbed and glucose dehydrogenase was immobilized.^{17,18} Katz et al. reported a compartment-less enzyme-based fuel cell with an operating voltage of 60 mV and a power density of 50 nW mm⁻².¹⁹ Katz et al. also proposed a “self-powered enzyme-based biosensor”, in which the current passing between a glucose-transport-limited anode and a cathode, not limited by O₂ transport, would be indicative of the glucose concentration. However, they did not address the essential issue of the source of the power for amplifying, measuring, and transmitting the signal from such a biosensor.²⁰ Tsujimura et al. reported a membrane-less glucose–O₂ biofuel cell operating in O₂-saturated 30 mM MOPS buffer in the presence of 50 mM glucose, producing 580 nW mm⁻² at an operating potential of 0.19 V.²¹ Chen et al. described a compartment-less biofuel cell

- (16) Kelley, S. C.; Deluga, G. A.; Smyrl, W. H. *AIChE J.* **2002**, *48*, 1071–1082.
 (17) Persson, B.; Gorton, L. *Enzyme Microb. Technol.* **1985**, *7*, 549–552.
 (18) Persson, B.; Gorton, L.; Johansson, G. *Bioelectrochem. Bioenerg.* **1986**, *16*, 479–483.
 (19) Katz, E.; Willner, I.; Kotlyar, A. B. *J. Electroanal. Chem.* **1999**, *479*, 64–68.
 (20) Katz, E.; Buckmann, A. F.; Willner, I. *J. Am. Chem. Soc.* **2001**, *123*, 10752–10753.
 (21) Tsujimura, S.; Kano, K.; Ikeda, T. *Electrochemistry* **2002**, *70*, 940–942.

based on the “wiring” of glucose oxidase and of laccase to 7- μ m-diameter, 2-cm-long carbon fiber electrodes.²² The output of their cell at 37 °C was 0.6 μ W, or 1.4 μ W mm⁻² at 0.38 V. Because their cathode was laccase-based, and because laccase loses much of its activity in 0.14 M NaCl and at pH 7.2,^{23–26} the cell had to be operated at pH 5 and in the absence of chloride. Mano et al. reported recently a laccase-comprising, compartment-less cell with an improved redox polymer connecting the reaction centers of glucose oxidase to the carbon fiber. It produced 1.2 μ W, or 2.7 μ W mm⁻², at an operating potential of 0.78 V, the highest reported for a miniature membrane-less biofuel cell.²⁷ Replacement of the laccase by bilirubin oxidase, an oxygen-electroreduction-catalyzing enzyme that maintains its activity at neutral pH and in the presence of 0.14 M NaCl,^{21,28–30} allowed operation of the “wired” enzyme-based compartment-less biofuel cell under physiological conditions. The cell produced 1.9 μ W at 37 °C under physiological conditions, or 4.3 μ W mm⁻² at 0.52 V at 37 °C. In its week-long operation, it generated 0.9 J of electrical energy while passing a charge of 1.7 C.³¹ If a zinc fiber of similar dimensions were utilized in a battery, and if the current efficiency of zinc utilization were 100%, only 0.005 C would have been passed. Thus, the dimensions of a biofuel cell operating for a week can be much smaller than those of a battery. Here we describe the characteristics of this membrane-less biofuel cell, showing that it produces electrical power when implanted in a living organism, a grape.

Experimental Section

Chemicals. Bilirubin oxidase (BOD) (EC 1.3.3.5, 1.3 U mg⁻¹) from *Trachyderma tsunodae* was purchased from Amano (Lombard, IL), and glucose oxidase (GOx) (EC 1.1.3.4, 191 U mg⁻¹) from *Aspergillus niger* was purchased from Fluka (Milwaukee, WI). Poly(ethylene glycol) (400 diglycidyl ether (PEGDGE) from Polysciences, Inc. (Warrington, PA), and NaIO₄ and NaCl from Sigma (St. Louis, MO), were used as received. A fresh solution of BOD in pH 7.4, 20 mM phosphate buffer (PB) was prepared daily. All solutions were made with deionized water passed through a purification train (Sybron Chemicals Inc., Pittsburgh, PA). The syntheses of the BOD-wiring redox polymer **II** (PAA-PVI-[Os(4,4'-dichloro-2,2'-bipyridine)₂Cl]⁺²⁺) and the GOx-wiring redox polymer **I** (PVP-[Os(N,N'-dialkylated-2,2'-biimidazole)₃]^{2+/3+}) were previously reported.^{28,29,31,32}

Instrumentation and Electrodes. The measurements were performed using a bipotentiostat (CH Instruments, Austin, TX, model CHI832) and a dedicated computer.

The 2-cm-long, 7- μ m-diameter carbon fiber electrodes (Goodfellow, Cambridge, UK) were contacted and coated by reported procedures.^{22,28,29,31,32} Each end of the fibers was cemented to a copper wire

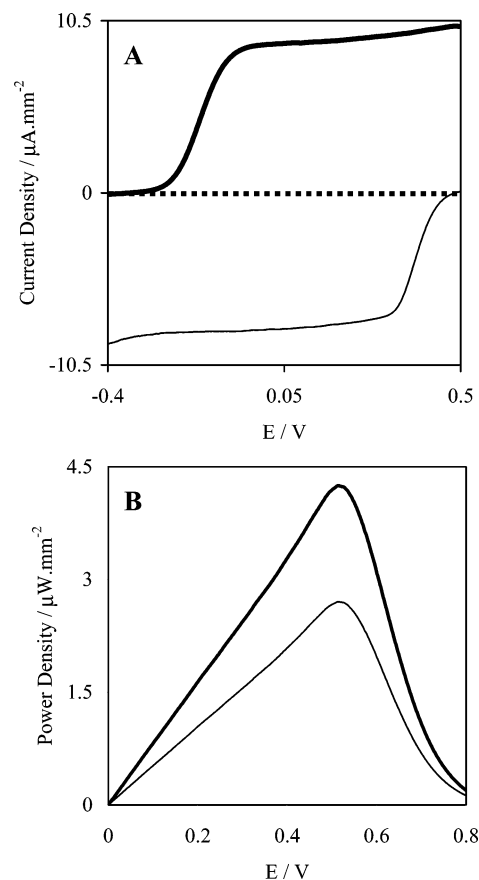


Figure 2. (A) Polarization of the anode (bold line) and of the cathode (fine line). (B) Dependence of the power density on the voltage of the cell at 25 °C (fine line) and at 37 °C (bold line). Quiescent solution in air, 37 °C, pH 7.2, 0.14 M NaCl, 20 mM phosphate, and 15 mM glucose.

using conductive carbon paint (SPI, West Chester, PA). The carbon paint was allowed to dry and then insulated with the epoxy. The active area of each fiber was 0.44 mm². Prior to their coating, fibers were made hydrophilic by exposure to a 1-Torr O₂ plasma for 3 min.³³ The cathodic catalyst was made, as described, of 44.6 wt % bilirubin oxidase, 48.5 wt % polymer **II**, and 6.9 wt % of the cross-linker PEGDGE.^{28,29,31} The anodic catalyst solution was made as follows: 100 μ L of 40 mg/mL of GOx in 0.1 M NaHCO₃ was oxidized by 50 μ L of 7 mg/mL of NaIO₄ in the dark for 1 h, and then 2 μ L of the periodate-oxidized GOx was mixed with 8 μ L of 10 mg/mL of polymer **I** and a 0.5- μ L droplet of 2.5 mg/mL of PEGDGE. A 5- μ L aliquot of this solution was applied to the carbon fiber. The resulting anodic catalyst consisted of the cross-linked adduct of 39.6 wt % GOx, 59.5 wt % polymer **I**, and 0.9 wt % PEGDGE. The glucose concentration was determined by using a FreeStyle blood glucose monitor (TheraSense Inc., Alameda, CA). The bulk cell used for the characterization of the electrodes in vitro had a Ag/AgCl (3 M KCl) reference electrode and a platinum wire counter electrode (BAS, West Lafayette, IN).

Implantation in the Grape. The fibers were implanted by making a pair of 2-cm-long cuts with a razor blade, so as to create a triangular groove and allow temporary removal of the cut part. After the fiber was implanted, the cut part was replaced in its groove.

Results

Figure 2A shows the polarization curves of the 7- μ m carbon fiber anode [modified with “wired” GOx (bold line)] and of the fiber cathode [modified with “wired” BOD (fine line)], in a quiescent 15 mM glucose solution in air at 37 °C in pH 7.2,

- (22) Chen, T.; Barton, S. C.; Binyamin, G.; Gao, Z.; Zhang, Y.; Kim, H.-H.; Heller, A. *J. Am. Chem. Soc.* **2001**, *123*, 8630–8631.
 (23) Barton, S. C.; Kim, H.-H.; Binyamin, G.; Zhang, Y.; Heller, A. *J. Phys. Chem. B* **2001**, *105*, 11917–11921.
 (24) Barton, S. C.; Kim, H.-H.; Binyamin, G.; Zhang, Y.; Heller, A. *J. Am. Chem. Soc.* **2001**, *123*, 5802–5803.
 (25) Barton, S. C.; Pickard, M.; Vasquez-Duhalf, R.; Heller, A. *Biosens. Bioelectron.* **2002**, *17*, 1071–1074.
 (26) Xu, F. *Appl. Biochem. Biotechnol.* **2001**, *95*, 125–133.
 (27) Mano, N.; Mao, F.; Shin, W.; Chen, T.; Heller, A. *Chem. Commun.* **2003**, 518–519.
 (28) Mano, N.; Kim, H.-H.; Zhang, Y.; Heller, A. *J. Am. Chem. Soc.* **2002**, *124*, 6480–6486.
 (29) Mano, N.; Kim, H.-H.; Heller, A. *J. Phys. Chem. B* **2002**, *106*, 8842–8848.
 (30) Tsujimura, S.; Tatsumi, H.; Ogawa, J.; Shimizu, S.; Kano, K.; Ikeda, T. *J. Electroanal. Chem.* **2001**, *496*, 69–75.
 (31) Mano, N.; Mao, F.; Heller, A. *J. Am. Chem. Soc.* **2002**, *124*, 12962–12963.
 (32) Kim, H.-H.; Mano, N.; Zhang, Y.; Heller, A. *J. Electrochem. Soc.* **2003**, *150*, A209–A213.

- (33) Sayka, A.; Eberhart, J. G. *Solid State Technol.* **1989**, *32*, 69–70.

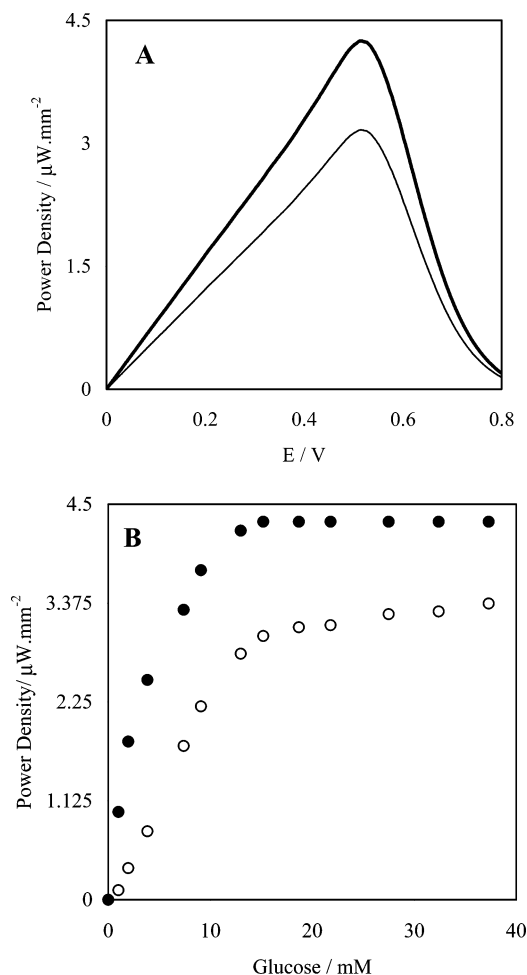


Figure 3. (A) Power output in air (bold line) and under oxygen (fine line). (B) Dependence of the power density on the glucose concentration of the cell in air (●) and under O₂ (○). The cell operates at +0.52 V. Conditions as in Figure 2.

0.14 M NaCl and 20 mM phosphate buffer solution. Catalytic electrooxidation of glucose was observed at -0.2 V vs Ag/AgCl, and it reached its plateau of $10 \mu\text{A mm}^{-2}$ near -0.1 V vs Ag/AgCl. Catalytic electroreduction of O₂ was observed at $+0.48$ V vs Ag/AgCl and reached its $9.5 \mu\text{A mm}^{-2}$ plateau near $+0.35$ V vs Ag/AgCl.

Figure 2B shows the power density of the biofuel cell at 25 °C (fine line) and at 37 °C (bold line). The dependence of the power output on the cell voltage in air (bold line) and under O₂ (fine line) is shown in Figure 3A. In the quiescent PBS buffer, the power density at 1 atm O₂ was 30% lower than that in air. Figure 3B shows the dependence of the power density on the glucose concentration in air (●) and under O₂ (○). The current density increased with the glucose concentration up to 20 mM, where a plateau of $4.4 \mu\text{W mm}^{-2}$ was reached in air and a plateau of $3.4 \mu\text{W mm}^{-2}$ was reached under O₂. At 2 mM glucose concentration, the power density was 80% lower under O₂ than it was in air; at 35 mM glucose concentration, it was 35% lower under O₂ than it was in air. Figure 4 shows the temperature dependence of the power density for the cell operating at +0.52 V in a quiescent solution in air at 37 °C in a pH 7.2, 0.14 M NaCl, 20 mM phosphate, and 15 mM glucose solution. The power density increased with temperature, reaching a plateau at 40 °C, and then declined above 50 °C.

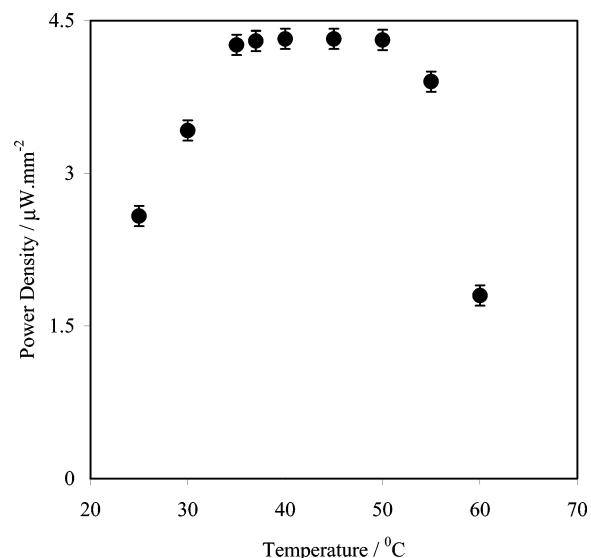


Figure 4. Temperature dependence of the power density of the cell operating at 0.52 V. Conditions as in Figure 2.

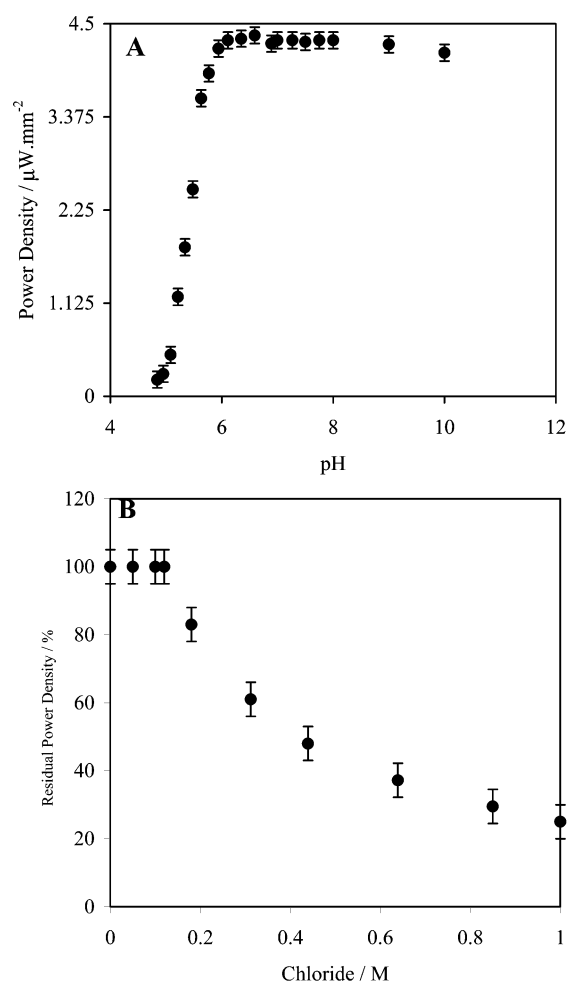


Figure 5. (A) pH dependence of the power density. (B) Dependence of the power density on the NaCl concentrations. Operating voltage +0.52 V. Conditions as in Figure 2.

The pH dependence of the power density for the cell operating at +0.52 V is seen in Figure 5A. The power density increased with pH, reaching a plateau at pH 6.2, and then declined slowly above pH 8.4. The NaCl concentration dependence of the power density for the cell operating at +0.52 V is shown in Figure

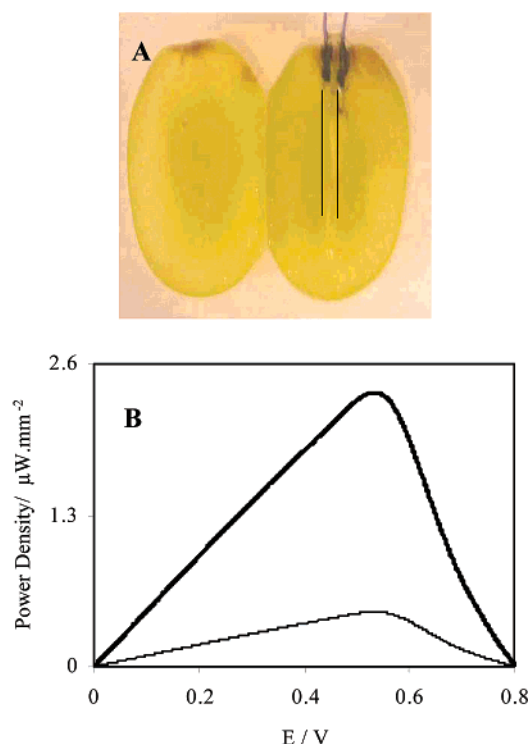


Figure 6. (A) Photographs of a whole and a sliced grape with the implanted fibers and their electrical contacts. Because in the photographs the 7- μm -diameter fibers were barely visible, lines are drawn to show their positions. (B) Dependence of the power output on the cell voltage with the cathode fiber implanted near the skin of the grape (bold line) and near the center of the grape (fine line).

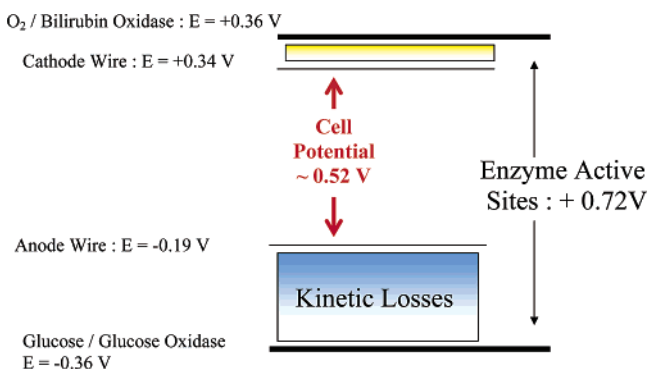
5B. The power was nearly independent of the NaCl concentration through the 0–0.1 M range and then declined, dropping at 1 M NaCl to one-fifth of its value at 0.1 M NaCl.

Implantation of the fibers in a grape (>30 mM glucose, pH 5.4), however, did yield an operating biofuel cell. Figure 6A shows a photograph of the sliced grape and the contacts of the implanted fibers. Because the fibers of 7- μm -diameter were barely visible in the photograph, lines representing their positions were drawn. The dependence of the power density on the operating voltage is shown in Figure 6B. The power output of the cell depended on the position of the cathode fiber. When the cathode fiber was located near the center of the grape, the power density was $0.47 \mu\text{W mm}^{-2}$; when the cathode fiber was near the skin of the grape, the power density was $2.4 \mu\text{W mm}^{-2}$. After 24 h of continuous operation, 78% of the initial power output was retained.

Discussion

The redox potential of GOx from *A. niger* at pH 7.2 is -0.32 vs Ag/AgCl,³⁴ and that of BOD from *T. tsunodae* is about $+0.36$ vs Ag/AgCl³⁵ (Scheme 2). Thus, when the cell operates at 0.52 V, the potentials of GOx and BOD differ by 0.72 V. This value, representing the limit of the operating voltage of the cell, is close to the difference between the observed threshold potentials for electrooxidation of glucose (-0.20 V vs Ag/AgCl) and electroreduction of oxygen ($+0.48$ V vs Ag/AgCl). Concentration polarization and overpotentials for the six electron-

Scheme 2. Operating Potentials (vs Ag/AgCl at pH 7.2) of the Enzymes and Their “Wiring” Redox Polymers



transfer steps of the anode and the cathode (Scheme 1) decrease the operating voltage at the point of maximum power to 0.52 V.

Redox polymer **I**, connecting the GOx reaction centers to the anode fiber, enables the electrooxidation of glucose at -100 mV vs Ag/AgCl at a current density of 1.1 mA cm^{-2} (Figure 2A, bold line),^{31,36} a potential only 260 mV oxidizing versus the estimated GOx redox potential at pH 7.3.³⁴ It differs from the earlier redox polymer³² in its redox center and in the tethering of its redox centers to the polymer backbone through a 13-atom-long flexible spacer arm. The redox potential of its $[\text{Os}(N,N'\text{-dialkylated-}2,2'\text{-biimidazole})_3]^{2+/3+}$ redox center is -190 mV vs Ag/AgCl, about 0.8 V reducing relative to that of the familiar $\text{Os}(\text{bpy})_3^{2+/3+}$ complex.^{31,36} Although the potential difference between the GOx redox centers and the redox polymer is only 170 mV, the polymer effectively wires the enzyme redox centers. The long tether binding the redox centers to the backbone reduces the overvoltage for driving the electrons from the GOx-FADH₂ centers to the redox polymer and through the polymer to the electrode. It provides for close approach of the redox centers of the polymer and of the enzyme and facilitates collisional electron transfer between neighboring polymer redox centers, as the tethered centers “wipe” the electrons from large overlapping proximal volumes of the hydrated cross-linked redox polymer.³¹

Redox polymer **II** is an electron-conducting redox copolymer of polyacrylamide and poly(*N*-vinylimidazole) complexed with $[\text{Os}(4,4'\text{-dichloro-}2,2'\text{-bipyridine})_2\text{Cl}]^{+/2+}$.^{28,29,31} It electrically wires the BOD $\text{Cu}^{+/2+}$ centers to the cathode fiber. As illustrated in Figure 2A (fine line), the overpotential for oxygen reduction to water is remarkably low. Even though the oxygen concentration in air-saturated pH 7 phosphate buffer is only about 0.1 mM, the current density of the oxygen cathode reaches 1.1 mA cm^{-2} at -220 mV vs the potential of the reversible $\text{O}_2/\text{H}_2\text{O}$ couple.^{28,29} Glucose is not electrooxidized on the cathode poised at $+0.4$ V vs Ag/AgCl.

When the anode and cathode fibers are of equal length, the currents of the two are equal when the anode is poised at -0.19 V vs Ag/AgCl and the cathode at $+0.33$ V vs Ag/AgCl, the cell operating at $+0.52$ V (Figure 2B). In a quiescent physiological buffer solution, the power output is $2.8 \mu\text{W mm}^{-2}$ at 25 °C (Figure 2B, fine line) and $4.4 \mu\text{W mm}^{-2}$ at 37 °C (Figure 2B, bold line).

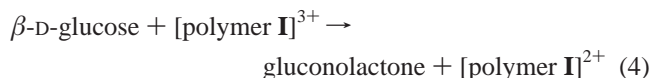
Oxygen Pressure Dependence. At low partial pressures of O_2 , where electroreduction of O_2 to water is O_2 mass-transport-

(34) Stankovich, M. T.; Schopfer, L. M.; Massey, V. *J. Biol. Chem.* **1978**, *253*, 4971–4979.

(35) Hirose, J.; Inoue, T.; Sakuragi, H.; Kikkawa, M.; Minakami, M.; Morikawa, T.; Iwamoto, H.; Hiromi, K. *Inorg. Chim. Acta* **1998**, *273*, 204–212.

(36) Mao, F.; Mano, N.; Heller, A. *J. Am. Chem. Soc.* **2003**, *125*, 4951–4957.

limited in the quiescent solution, the power increases with the partial pressure of O₂ until the kinetic limit of the cathodic electrocatalyst is reached. As the O₂ partial pressure is increased, the anodic glucose electrooxidation current decreases, because O₂ competes with the “wire” for GOx FADH₂ electrons (eqs 4 and 5). As can be seen in Figure 3A, at 37 °C and 15 mM glucose concentration, switching the bubbled gas from air to oxygen results in the loss of one-third of the power when the cell operates at 0.52 V.



As illustrated in Figure 3B, the loss depends on the glucose concentration. Although above 15 mM glucose concentration about one-third of the power is lost when the atmosphere is switched from air to oxygen, the loss is much greater, four-fifths of the output, at 2 mM glucose concentration. The difference is attributed to the slower electrooxidation of the solution side of the film than its electrode side. At high glucose concentration, the glucose-reduced front moves toward the electrode, and the effective kinetic resistance is reduced. Excessive loss of current by electroreduction of O₂ at the glucose-oxidizing anode is avoided because of the rapid diffusion of electrons in GOx “wiring” redox polymer I (Scheme 1); the apparent electron diffusion coefficient is as high as $5.8 \times 10^{-6} \text{ cm}^2 \text{ s}^{-1}$.^{31,36} The redox centers of the film are rapidly electrooxidized even at -0.1 V vs Ag/AgCl, and in an aerated solution most of the electrons of GOx are captured by polymer I rather than by dissolved O₂.

While the H₂O₂ produced in the competing side reaction of O₂ with reduced glucose oxidase could damage the glucose electrooxidizing anode if the H₂O₂ were allowed to accumulate, the damage it causes to the anode when diluted or decomposed by catalase, an abundant enzyme in many organisms, is not significant.³⁷

Temperature Dependence. The temperature dependence of the cell operating at 0.52 V at 15 mM glucose concentration in a quiescent PBS buffer solution in air and at 37 °C is seen in Figure 4. The power density increases up to 50 °C and then declines rapidly as one or both of the enzymes are denatured. The activation energies are 28.3 kJ mol⁻¹ for the anode reaction³¹ and 34.3 kJ mol⁻¹ for the cathode reaction.²⁸ At ambient temperature, the power density is limited by the kinetics of the cathodic bioelectrocatalyst. The observed activation energy for the thermal denaturing of bilirubin oxidase is 88.2 kJ mol⁻¹, and for glucose oxidase it is 96 kJ mol⁻¹.^{28,38} Even though the activation energy for denaturing glucose oxidase is higher, it is the denaturing of bilirubin oxidase²⁸ that causes the observed decline from 4.5 to 3.45 $\mu\text{W mm}^{-2}$ upon increasing the temperature from 45 to 55 °C at a rate of 10 °C/h, because in this temperature domain the power output is controlled by the cathode in the 15 mM aerated glucose solution. Because both enzymes are denatured and the activation energy for the denaturing of GOx exceeds that of BOD,^{28,38} at temperatures above 55 °C the cell becomes anode-limited, and heating at a

rate of 10 °C/h from 55 to 60 °C causes the power to drop rapidly, from 3.45 to 2.0 $\mu\text{W mm}^{-2}$.

pH Dependence. Figure 5A shows the pH dependence of the power density when the cell operates at +0.52 V in air. The current density of the anode is near its maximum between pH 6 and 8.2.³⁸ The current density of the cathode is nearly independent of pH in the pH 6–10.5 range.^{28,29} At pH < 6,^{28,29,38} the power is limited by the kinetics of the anode; at pH 5, where the current density of the anode is 2.0 $\mu\text{A mm}^{-2}$ and that of the cathode is 4.5 $\mu\text{A mm}^{-2}$, the power density drops to 1.0 $\mu\text{W mm}^{-2}$. As the pH is raised to pH 6, the kinetics of the anode improves and, as shown in Figure 5A, the power density increases.³⁸ Above pH 6, the current of the cathode is lower than that of the anode. At pH 7,³¹ where the anode current density is 12 $\mu\text{A mm}^{-2}$ and the cathode current density is 10 $\mu\text{A mm}^{-2}$, the cathode controls the power. Thus, the optimal operating pH for the cell consisting of two carbon fibers of equal length is 6. Above pH 8.4, the power decreases because of denaturation of bilirubin oxidase.^{28,29} In the pH range of human serum or blood (pH 7.1–7.4), the variation in power is negligibly small.

Effect of NaCl. Serum, blood, and other physiological fluids contain 0.14 M chloride. Copper-binding anions, particularly halide anions, inhibit multi-copper oxidases. In addition, the electrostatic bond between the polyanionic enzyme and the polycationic redox polymer, which prevents their phase separation, is weakened at high ionic strength, where the enzyme and polymer charges are screened by their respective counterions.^{15,39,40} At greater cross-linking, the phase separation is reduced. The dependence of the power output on the NaCl concentration is seen in Figure 5B. Above 0.15 M, the anodic current monotonically declines upon increasing the NaCl concentration. Because increasing the salt concentration from 0.1 to 1 M decreases the current density of the “wired” BOD cathode only by 2%,^{28,29} the decrease in the power output is attributed to the partial unwiring of the GOx.³⁸

Operation in the Grape. For the experiment demonstrating that the cell consisting merely of two coated carbon fibers actually operates in a living organism, we implanted the cell in a grape, a fruit containing >30 mM glucose in its sap. The power output of the cell functioning in the grape was O₂-transport-controlled and depended on the position of the cathode fiber. When the cathode fiber was near the center of the grape, where the fruit was oxygen-deficient, the power density was only 0.47 $\mu\text{W mm}^{-2}$ at 0.52 V. When the fiber was shallowly implanted near the skin of the grape, where the sap was better oxygenated, the power density was 2.4 $\mu\text{W mm}^{-2}$ at 0.52 V.

Conclusion

The area of the electrodes of the compartment-less glucose–O₂ biofuel cell, consisting of two electrocatalyst-coated 7- μm -diameter, 2-cm-long carbon fibers, is 180 times smaller, its operating voltage is 8 times higher (0.52 vs 0.06 V), and its power density 12 times higher (4.3 vs 0.35 $\mu\text{W mm}^{-2}$) than those of an earlier reported compartment-less glucose–O₂ cell which also operated under physiological conditions.¹⁹ At neutral pH, where the power output of the cell is cathode-limited, the activation energy for power increase is 34.3 kJ mol⁻¹. Above

(37) Binyamin, G.; Heller, A. *J. Electrochem. Soc.* **1999**, *146*, 2965–2967.

(38) Mano, N.; Mao, F.; Heller, A. Unpublished results, 2003.

(39) Degani, Y.; Heller, A. *J. Am. Chem. Soc.* **1989**, *111*, 2357–2358.

(40) Katakis, I.; Ye, L.; Heller, A. *J. Am. Chem. Soc.* **1994**, *116*, 3617–3618.

50 °C, the decline is caused by the thermal denaturing of bilirubin oxidase, having an activation energy of 88.2 kJ mol⁻¹. When the lengths of the anode and cathode fibers are the same, the power output is limited in the aerated solution below pH 6 by the anode and above pH 6 by the cathode. In the pH range of human serum or blood, the variation of power output is negligibly small. The power output does not vary substantially with NaCl concentration in the 0.05–0.15 M range; in the 0.15–1 M range it declines as the NaCl concentration is raised. The cell operates continuously at 37 °C in an aerated, glucose-containing physiological (pH 7.2, 0.14 M NaCl, 20 mM phosphate) buffer for a week,³¹ and, as shown here, it retains 78% of its initial power output of 1.1 μW after operating for a day in a living organism, a grape. The power output of the cell at 37 °C in a physiological buffer solution is 1.9 μW, sufficient for powering low-power CMOS circuits,⁴¹ and its operating voltage of 0.52 V is adequate for operation of low-voltage CMOS/SIMOX integrated circuits.⁴² We hope, that after considerable further development, the simple and disposable cell will power implanted autonomous sensor–transmitter systems

of relevance to physiological research and medicine. These miniature systems could monitor, for example, the temperature at a site following surgery, indicative of inflammation.

Acknowledgment. We thank Dr. Hyug-Han Kim for the synthesis of polymer **II**. The study was supported in part by the Office of Naval Research (grant no. N00014-02-1-0144) and by the Welch Foundation.

Note Added after ASAP. In the article posted ASAP April 30, 2003, there were several errors. The last two sentences in the abstract have been changed; the first paragraph in the Introduction now reads “platinum group metal catalysts, without a membrane”; in the paragraph headed **Instrumentation and Electrodes** PESDGE now reads PEGDGE; in the first paragraph of the Discussion the first two sentences have been changed; in the third paragraph –140 mV has been changed to –220 mV; the title of Scheme 2 has been changed; and in the paragraph headed **Operation in the Grape** changes were made to eliminate the reference to the grasshopper. The final version published on the Web May 13, 2003, and the print version are correct.

JA0346328

(41) Harrison, R. R.; Koch, C. *Analog Integr. Circuits Signal Process.* **2000**, *24*, 213–216.

(42) Harada, M.; Tsukahara, T.; Kodate, J.; Yamagishi, A.; Yamada, J. *IEEE J. Solid State Circuits* **2000**, *15*, 2000–2004.